

SEISMIC POUNDING ANALYSIS OF ADJACENT REINFORCED CONCRETE BUILDINGS

R.M.Khattab¹, M.T. El-Sheikh², and N.A.Yehia²

Seismic pounding between adjacent buildings may occur during earthquakes, if the separation between them is insufficient. This paper studies the seismic pounding between two reinforced concrete moment resisting frame buildings. Two cases are selected depending on the relative story heights between the two buildings. Case 1 is called floor-to-floor buildings, where story height is equal for the two buildings. Case 2 is called floor-to-column buildings, where story heights may vary between the two buildings. Energy dissipation during collisions is considered by using a gap element together with a link element with both stiffness and viscous damping properties. Finite element analysis software DRAIN 2DX is used to analyze the buildings. The structural elements of the buildings are designed to fulfill the Egyptian code requirements. Eleven earthquake records are used as input ground motions to investigate the response of buildings. Impact forces, displacements, and end column shear are computed to evaluate the performance of the buildings. Floor-to-column pounding during earthquakes results in a non-uniform and chaotic distribution of end column shear along the building height. Also, the maximum end column shear force locates below the positions of pounding, which contradicts the position of design maximum shear at the building base.

Keywords: Seismic pounding; adjacent buildings; pounding force; Gap element; floor-to-column.

1- INTRODUCTION

Seismic pounding is defined as the collision of adjacent buildings during earthquakes. The principal reason for seismic pounding is insufficient separation between the buildings. The most significant manifestation of pounding hazard was reported in Mexico City, due to the 1985 Mexico earthquake where 15% of all cases led to collapse [Rosenblueth and Meli, 1986]. Many studies were made about structural pounding. [Karayannis and Favvata, 2005] studied the influence of structural pounding on the ductility requirements and seismic behaviour of reinforced concrete structures with equal and non-equal heights. Idealized models with a lumped mass system were considered using the program DRAIN-2DX for the analysis. [Rahman *et al.*, 2001] highlighted the influence of soil flexibility effects on seismic pounding for adjacent multi-story buildings of differing total heights. [Cole *et al.*, 2010] studied the employ wave theory to calculate the pounding forces or that combines both buildings as a single unit during collisions.

[Muthukumar and Desroches, 2006] studied Stereo-mechanical, linear spring, Kelvin, Hertz contact

1- Ph.D. Student, Faculty of Engineering, Cairo University, Egypt

2- Structural Engineering Department, Faculty of Engineering, Cairo University, Egypt

models and presented a model with non-linear damping which is based on Hertz contact model.

[AbdelRaheem, 2006] used three types of ground acceleration records for obtaining seismic pounding behaviour of adjacent buildings. [Westermo, 1989] presented a method for preventing pounding damages of adjacent buildings by using dampers which are placed between joints of adjacent buildings. Also [Matsagar and Jangid, 2005] presented a method for damping pounding forces by using viscoelastic dampers. [Maison *et al.*, 1990] analyzed pounding of adjacent multi-degree-of-freedom structures by classifying pounding types and made calculations of pounding cases at different floor levels. [Anagnostopoulos, 1988] modelled four adjacent single-degree-of-freedom structures and studied pounding behaviour.

In another study of [Anagnostopoulos, 1992], five ground acceleration records were used and variables which change character of pounding. [Sayed *et al.*, 2005] used Different multi-degrees-of-freedom (MDOF) models in the two and three dimensions (2-D & 3-D) with linear and nonlinear behaviour to idealize the adjacent buildings.

2- FINITE ELEMENT MODELLING

2-1- Building modelling

This study investigates pounding of adjacent building structures. A simplified nonlinear model of a multi-story building is developed. A two-dimensional (2D) finite element frame has been defined and non-linear time-history analyses have been performed. DRAIN-2DX program [Prakash *et al.*, 1993] is used for analysis. The elastic design of the prototype frames was made in accordance with the Egyptian Code [ECP-203, 2007]. Six groups of two buildings were selected according to the height of the two buildings. The first group G_{10-5} , building 1 is 10 stories and building 2 is 5 stories. The second group G_{15-5} , building 1 is 15 stories and building 2 is 5 stories. The third group G_{15-10} , building 1 is 15 stories and building 2 is 10 stories. The fourth group G_{20-5} , building 1 is 20 stories and building 2 is 5 stories. The fifth group G_{20-10} , building 1 is 20 stories and building 2 is 10 stories. The sixth group G_{20-15} , building 1 is 20 stories and building 2 is 15 stories. For all groups, two cases were considered in this study. Case1 floor-to-floor; means that the two buildings have the ground floor height equal to 5.0 m and the typical story height equal to 3.0 m. Case 2 floor-to-column; the tall building ground floor height is equal to 5.0 m

while it is equal to 6.50 m in the lower building and the typical story height for both buildings is 3.0 m. Example for two building; case1 and case2 is shown in Figs. (1a, b). Concrete with compressive strength $f_{cu} = 25 \text{ N/mm}^2$, unit weight $\gamma = 25 \text{ kN/m}^3$, modulus of elasticity $E = 24,281 \text{ N/mm}^2$, and Poisson's ratio $\nu = 0.2$ and reinforcing steel with yield strength $f_y = 360 \text{ N/mm}^2$ are used for analysis and design. Live load of 2 kN/m^2 , roof load of 1 kN/m^2 and partition wall load of 1 kN/m^2 are considered in analysis. Cross section area of beams and columns of buildings are given in Table 1. The building mass considered in the dynamic analyses is the seismic weight W (i.e., the total dead load and applicable portions of other loads) divided by the acceleration of gravity, g . The building mass is equally divided between the two lateral resisting frames. The mass assigned to each frame is distributed in proportion to the floor and roof weight and lumped at the floor and roof levels. Therefore, the first floor mass is bigger than the rest of the floor masses and the roof mass is smaller. However, the vertical distribution of the mass is very close to uniform. Each floor or roof mass is equally distributed between the nodes at the centreline intersections of beams and columns of each floor or roof level.

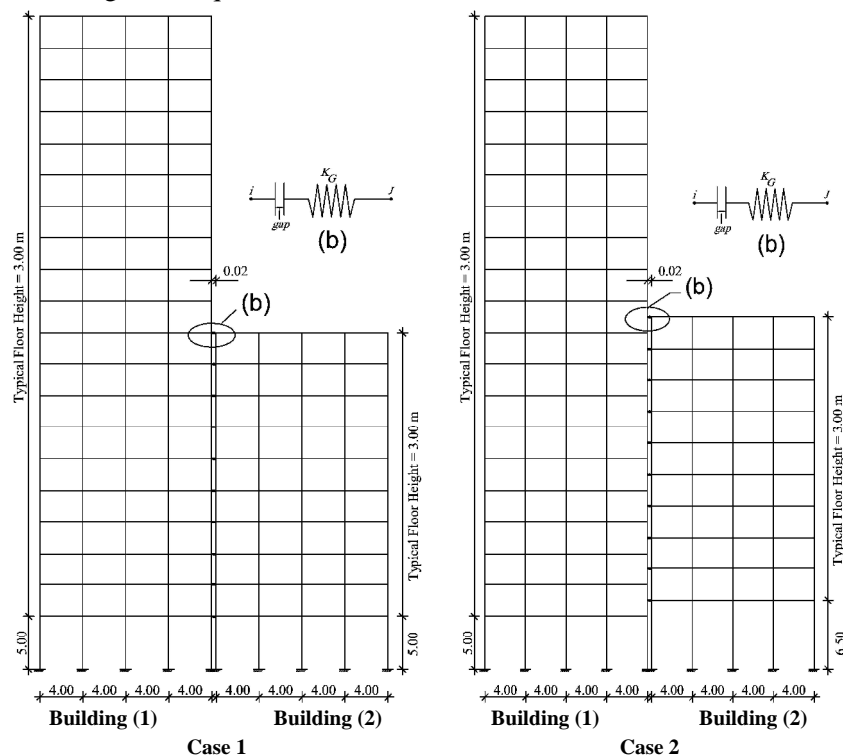


Fig.1- Example for Two Buildings Used, Case1 Floor-to-Floor; Case2 Floor-to- Column,
(b) Gap Element Type

Table 1- Cross Section Area and Reinforcement for Beams and Columns

Name of Buildings	Element Type	1 st Floor to 5 th Floor	6 th Floor to 10 th Floor	11 th Floor to 15 th Floor	16 th Floor to 20 th Floor
5-Story Buildings	Beams	300x600 mm	-	-	-
	Columns	350x700mm	-	-	-
10-Story Buildings	Beams	300x600mm	300x600mm	-	-
	Columns	350x800mm	300x700mm	-	-
15-Story Buildings	Beams	300x700mm	300x700mm	300x600mm	-
	Columns	400x900mm	350x800mm	300x700mm	-
20-Story Buildings	Beams	300x800mm	300x800mm	300x700mm	300x700mm
	Columns	500x1100mm	400x1100mm	400x1000mm	300x1000mm

2-2- Modelling of viscous damping

Damping of the prototype frames is modelled as viscous damping. The viscous damping is assumed mass and stiffness proportion. The mass and stiffness proportional factors are (α , β) calculated according to [Clough and Penzien, 1993] using

$$\begin{Bmatrix} \alpha \\ \beta \end{Bmatrix} = \frac{2\omega_m \omega_n}{\omega_n^2 - \omega_m^2} \begin{bmatrix} \omega_n & -\omega_m \\ -1/\omega_n & 1/\omega_m \end{bmatrix} \begin{Bmatrix} \xi_m \\ \xi_n \end{Bmatrix} \quad (1)$$

Where

ξ_m & ξ_n are critical damping ratios for the m-th and n-th modes of vibration,

ω_m & ω_n are natural frequencies for the m-th and n-th modes of vibration.

For calculating damping factors, the modes of each prototype frames should be first calculated. Then we assume damping for modes number one and three equal to 0.05 of the critical damping, which is usually used for concrete structures.

2-3- GAP Modelling

Gap device response was modelled using DRAIN-2DX [Prakash *et al.*, 1993] element type 09, which allow for a tri-linear axial response definition. The element formulation also allows for inelastic unloading. In this study elastic unloading was used for gap definition. The theoretical response of element type 09 used in this study is illustrated in (Figs.2a and b) the gap element was defined by providing two stiffness values (K_1 , K_2) and two transition displacement values (u_1 and u_2). Elastic or viscous-elastic impact elements are often used to model pounding between adjacent structures, however, Kelvin-Voigt element (i.e. a linear spring-damper element) is mostly used to model impact between two colliding structures.

The viscous component of the Kelvin-Voigt element dissipates energy throughout the approach and restitution period, but in reality, most of the energy dissipation takes place during the approach period and minor energy dissipation is observed during restitution period. However, for simplicity,

to simulate structural pounding the Kelvin-Voigt element has been widely used. The force in the Kelvin-Voigt element $F(t)$ during impact is given by

$$F(t) = K_L \delta(t) + C_L \dot{\delta}(t) \quad (2)$$

Where

$\delta(t)$ is relative displacement of colliding structural elements,

$\dot{\delta}(t)$ is relative velocity between colliding elements,

K_L is stiffness, and

C_L is damping coefficient and is given by

$$C_L = -2 \ln e_r \sqrt{\frac{K_L m_1 m_2}{[\pi^2 + (\ln e_r)^2] (m_1 + m_2)}} \quad (3)$$

Where e_r is coefficient of restitution, m_1 and m_2 are masses of structural members [Anagnostopoulos, 1988]. Building pounding researchers usually express collision damping in terms of the coefficient of restitution; e_r . Recommended value of e_r ranges from 1.0 to 0.4, however typically 0.65 is used by [Mouzakis and Papadrakakis, 2004; Shakya and Wijeyewickrema, 2009]. Numerical simulation performed by [Jankowski, 2005] showed that for concrete-to-concrete impact, $K_L = 93,500$ kN/m and $e_r = 0.65$ provides good correlation between experimental results provided by [Van Mier *et al.*, 1991] and theoretical results. Pounding between buildings is simulated using Gap elements as shown in Fig. (2).

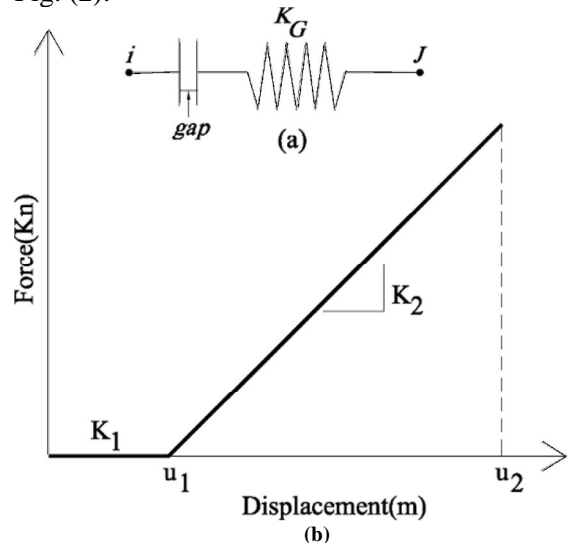


Fig. 2- (a) Gap Element, (b) Link Element Force-Displacement Relationship

The force transmits from one structure to another only when contact occurs.

The force-deformation relationship of the gap element is given by

$$f_G = \begin{cases} K_G [(u_i - u_j) - \text{gap}] & \text{if } u_i - u_j > \text{gap} \\ 0 & \text{if } u_i - u_j < \text{gap} \end{cases} \quad (4)$$

Where

f_G is force,

K_G is spring constant,

u_i and u_j are nodal displacements of nodes i and j , and gap is initial gap opening in this study is equal to 2.0 cm. the stiffness of gap element K_G is considered as $100K_L$ to ensure that it works nearly rigidly when the gap is closed.

2- 4- Selected Ground Motions

A total of eleven earthquake ground motions have been selected for this study, five of them are natural ground motions while the remaining six are generated ground motions.

The natural ground motions are chosen to represent different site soil conditions. Since prototype frames are designed for medium soil, three of the five natural ground motions are for this site soil condition. The other two soil types are represented by only one natural ground motion. The most important characteristics of the five selected natural ground motion records are given in Table 2.

The generated ground motions are generated from either a given power spectrum or compatible with a given response spectrum (usually a certain design response spectrum). The acceleration time-histories of the earthquake records are scaled to have a PGA of 0.15g.

Table 2- General Characteristics of Selected Natural Ground Motions

Earthquake	Year	Station	PGA(g)	Site Class	Record Name
Loma Prieta, USA	1989	Foster City	0.28	Soft	FOS
Loma Prieta, USA	1989	Hollister South Street	0.369	Medium	HOLL
Landers, USA	1992	Yermo, Ca.	0.24	Medium	YER
Northridge, USA	1994	Newhall, Ca.	0.593	Medium	NEWH
Imperial Valley, USA	1940	El Centro	0.35	Stiff	ELC

3- NUMERICAL ANALYSIS AND RESULTS

3-1- Impact force

The different magnitudes of pounding forces for selected ground motions at roof level of the lower building for the two cases are shown in Figs. (3a,b,c,d,e, and f).

The maximum value of pound-ing force for case1 occurs at GENSOFF1 for all groups. For the same case, the minimum value of pounding force occurs at ELC for groups G_{10-5} , G_{15-10} , G_{20-5} , and G_{20-10} , and at GENROCK1 for G_{15-5} , and G_{20-15} . For case2, the maximum value of pounding force occurs at GENSOFF1 for groups G_{20-5} , G_{20-10} , and G_{20-15} and at FOS for G_{15-5} and G_{15-10} and for G_{10-5} at SOF1. For the same case the minimum value of pounding force occurs at ELC for groups G_{10-5} , G_{15-10} , G_{20-5} , and G_{20-10} , and at GENROCK1 for G_{15-5} , and G_{20-15} .

The maximum percentage of difference in pounding force between the two cases is 42%, 37%, and 25% for groups G_{10-5} , G_{20-15} , and G_{20-10} respectively at STF1 ground motion and 46%, and 30% for groups G_{15-10} and G_{20-5} , respectively at GENMED1 ground motion and 39% for G_{15-5} at GENROCK1 ground motion.

The minimum percentage of difference in pounding force between the two cases is 8%, 13%, 15%, and 18% for groups G_{20-5} , G_{15-10} , G_{20-15} , and G_{10-5} , respectively at ELC ground motion and 8% for groups G_{20-10} at GENROCK1 ground motion and 2.5% for G_{15-5} at FOS ground motion. Generally for both cases and for generated earthquake, the maximum value of pounding force is for GENSOFF1 and SOF1 and the minimum value of pounding force is for GENROCK1 and STF1.

3-2- Displacement

The absolute value of roof displacement for all groups, both cases according to all selected ground motions are summarised in Table 3 and Table 4 for tall and short buildings, respectively. From results, the maximum roof displacement for taller buildings at both cases occurs at GENSOFF1, and SOF1.

The percentage of difference in tall building maximum roof displacement between the two cases is 3.6%, 4.5%, 4.1%, 3.7%, 4.1%, and 3.1% for groups G_{10-5} , G_{15-5} , G_{15-10} , G_{20-5} , G_{20-10} , and G_{20-15} , respectively.

The maximum roof displacement for short building at both cases occurs at GENSOFF1 and SOF1 except for group G_{15-10} at FOS. The percentage of difference in short building maximum roof displacement between the two cases is 11.7%, 8.5%, 9.7%, 12.1%, 13.1%, 9.3% for groups G_{10-5} , G_{15-5} , G_{15-10} , G_{20-5} , G_{20-10} and G_{20-15} , respectively.

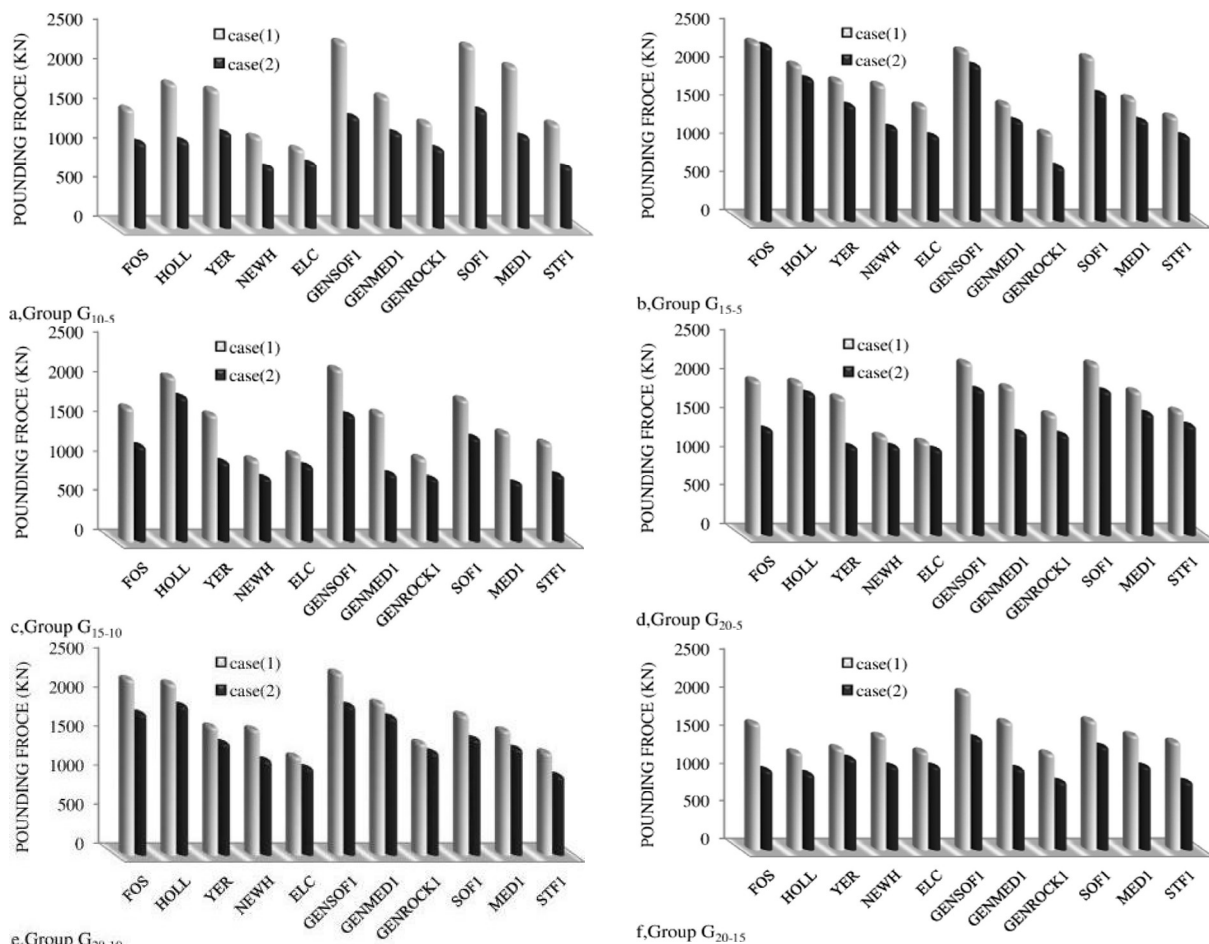


Fig 3 - Pounding Force for Selected Ground Motions at Roof of Lower Building

Table 3 - Tall Buildings' Roof Displacement (cm)

RQ Record	G _{10.5} (U10)		G _{15.5} (U15)		G _{15.10} (U15)		G _{20.5} (U20)		G _{20.10} (U20)		G ₁₂₋₁₅ (U20)	
	Case 1	Case 2	Case 1	Case 2	Case 1	Case 2	Case 1	Case 2	Case 1	Case 2	Case 1	Case 2
FOS	13.0	13.3	15.6	16.0	16.6	16.7	15.3	15.9	15.1	15.7	15.2	15.7
HOLL	11.5	11.6	16.0	16.1	16.2	16.4	16.5	16.7	16.5	16.9	16.5	17.5
YER	10.8	10.8	10.1	10.1	10.5	10.9	12.3	12.6	13.0	14.3	12.9	13.6
NEWH	8.9	9.0	8.1	9.9	8.9	9.9	12.1	12.2	12.3	12.5	12.8	13.6
ELC	9.8	9.9	10.7	10.7	10.8	10.7	11.7	11.9	12.1	12.3	12.4	13.1
GENSO F1	14.3	14.9	14.7	15.3	15.2	15.8	20.6	20.9	22.0	22.7	20.0	21.0
GENMD 1	8.1	9.6	13.1	14.0	13.4	13.6	17.1	17.8	16.7	17.9	15.8	17.0
GENROCK1	8.4	8.5	9.2	10.2	10.2	10.6	10.2	10.3	10.4	11.4	9.7	10.5
SOF 1	12.0	12.7	17.1	17.9	17.4	18.1	20.7	21.4	22.1	23.0	21.7	22.4
MED 1	9.1	9.5	15.0	15.5	15.0	15.6	16.5	17.4	16.8	17.1	15.6	16.2
STF 1	7.7	8.2	10.1	10.2	11.0	11.9	12.0	12.9	11.3	12.7	10.9	12.0

Table 4 - Short Buildings' Roof Displacement (cm)

RQ Record	G _{10.5} (U5)		G _{15.5} (U5)		G _{15.10} (U10)		G _{20.5} (U5)		G _{20.10} (U10)		G ₁₂₋₁₅ (U15)	
	Case 1	Case 2	Case 1	Case 2	Case 1	Case 2	Case 1	Case 2	Case 1	Case 2	Case 1	Case 2
FOS	8.5	9.3	8.6	9.4	10.0	10.9	8.9	9.9	9.8	10.6	14.3	15.0
HOLL	7.2	9.5	6.1	7.5	10.5	10.7	8.1	9.5	9.5	9.9	15.0	15.8
YER	8.4	7.9	8.7	8.8	8.1	8.8	8.1	8.4	10.7	10.8	10.5	11.2
NEWH	5.6	6.5	6.1	6.5	5.4	7.0	7.0	7.5	8.9	9.0	9.6	10.0
ELC	4.6	6.0	4.9	5.5	9.1	9.9	4.3	5.4	8.0	8.6	9.1	9.8
GENSO F1	9.7	10.8	9.0	9.3	10.6	10.8	6.3	7.5	9.9	10.5	17.9	18.2
GENMD 1	4.2	5.8	4.3	5.5	9.0	9.6	4.2	5.0	9.5	10.3	11.5	12.1
GENROCK1	3.6	4.9	3.7	4.9	8.3	9.2	3.7	4.9	7.9	9.3	9.2	10.2
SOF 1	8.1	9.2	9.9	10.8	10.8	11.9	9.0	10.1	11.1	12.5	18.2	19.9
MED 1	6.4	7.9	7.6	8.9	9.1	9.2	8.0	9.2	10.3	11.3	16.2	16.9
STF 1	4.5	4.8	3.9	4.6	6.6	8.8	3.4	4.5	5.8	7.4	9.2	9.9

3-3- End Column Shear

The most elements affected during buildings pounding are columns and specially the end columns (columns adjacent to each others on the contact line between the two buildings). Pounding between buildings produces shear force.

Three groups are selected to represent the end column shear force.

Figs. (4, 5, and 6) show the end column shear force for taller building in groups G_{20-5} , G_{20-10} and G_{20-15} respectively.

The maximum shear forces for group G_{20-5} occur at GENSOF1 for both cases.

For case 1 the maximum shear force is about 34 kN and located at the ground floor but for case 2 the maximum shear force is about 63 kN and located at the sixth floor.

The maximum shear forces for group G_{20-10} occur at SOF1 and GENSOF1 for case1 and case2, respectively.

For case1 the maximum shear force is about 29 kN and located at the ground floor but for case2 the maximum shear force is about 62 kN and located at the eleventh floor.

The maximum shear forces for group G_{20-15} occur at SOF1 and GENSOF1 for case1 and case2, respectively.

For case1 the maximum shear force is about 28 kN and located at the ground floor but for case2 the maximum shear force is about 34 kN and located at the sixteenth floor.

According to end column design for case2, shear force due to pounding between two buildings exceeds the shear capacity of the columns.

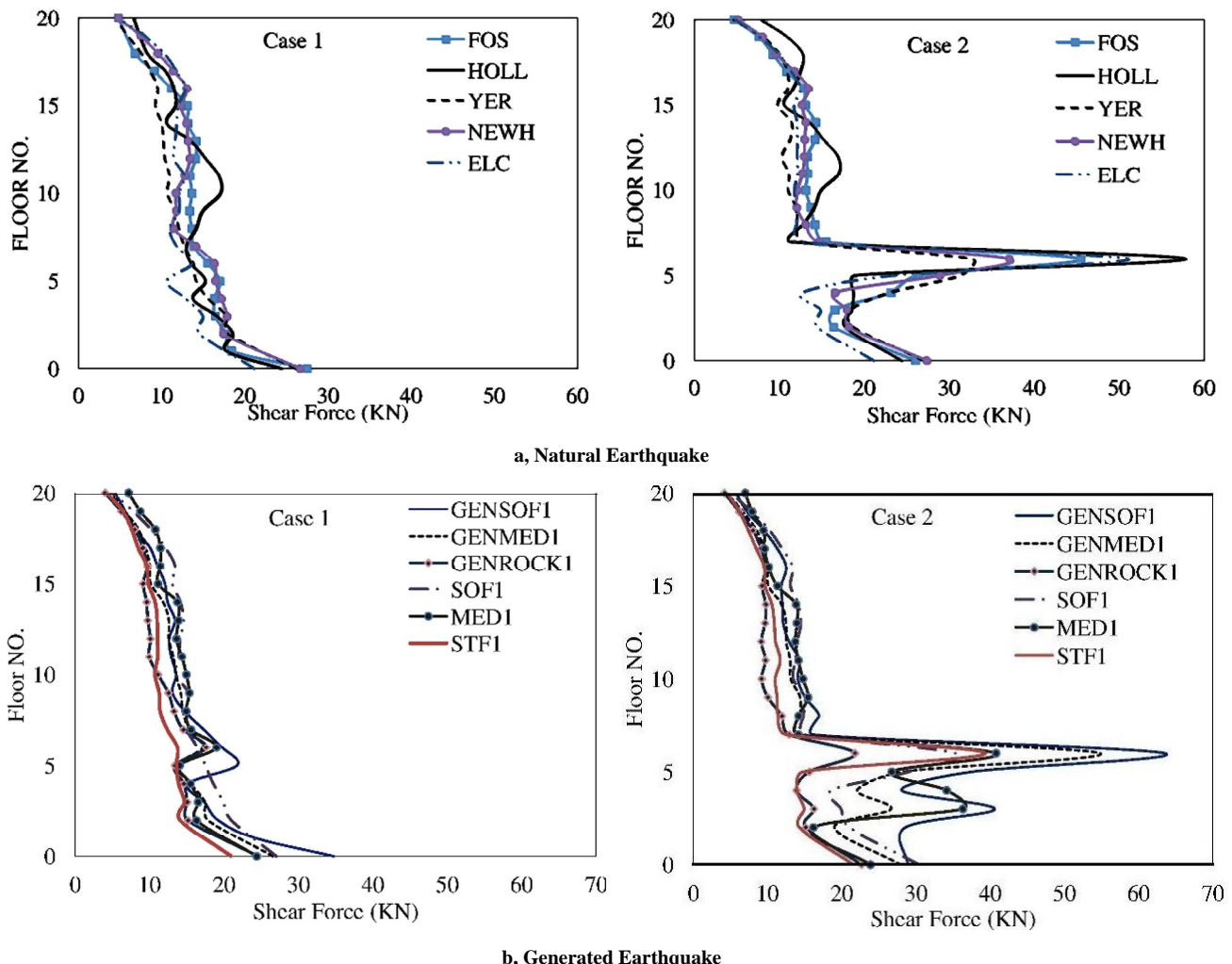


Fig. 4 - End Column Shear Force for group G_{20-5} Due to Selected Earthquake

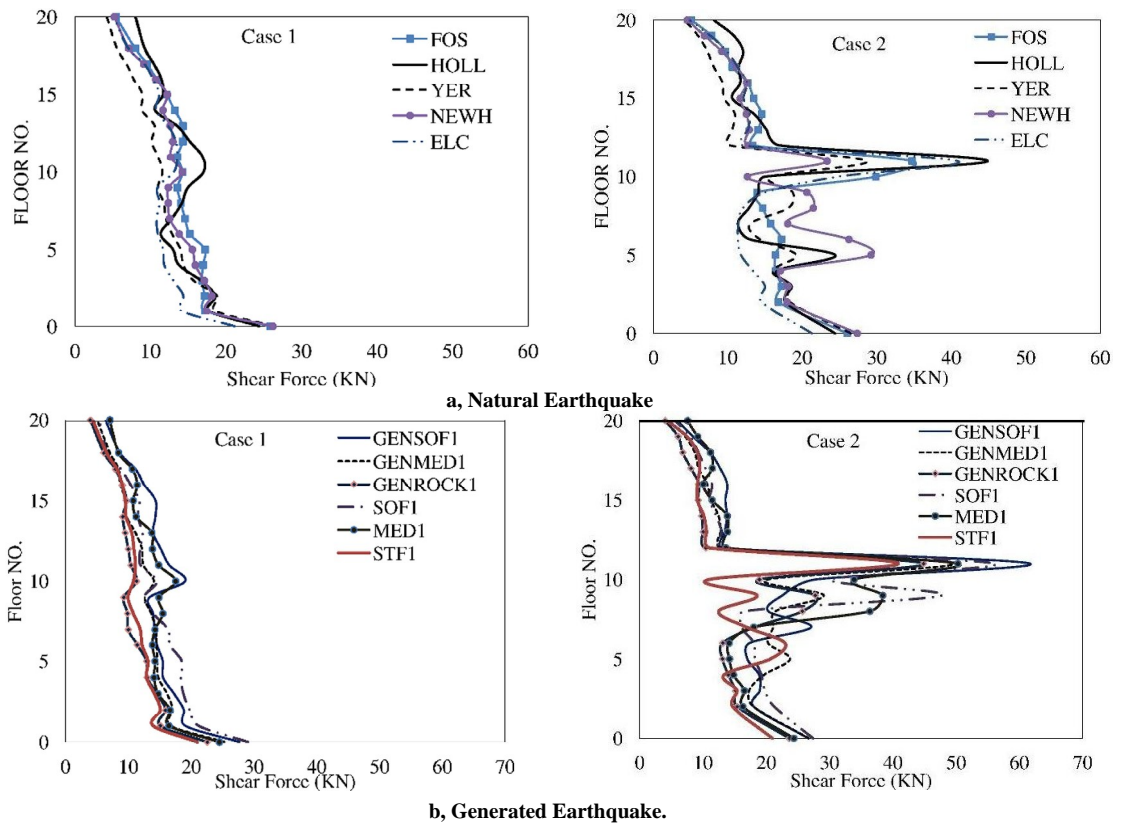


Fig. 5 - End Column Shear Force for Group G_{20-10} Due to Selected Earthquake

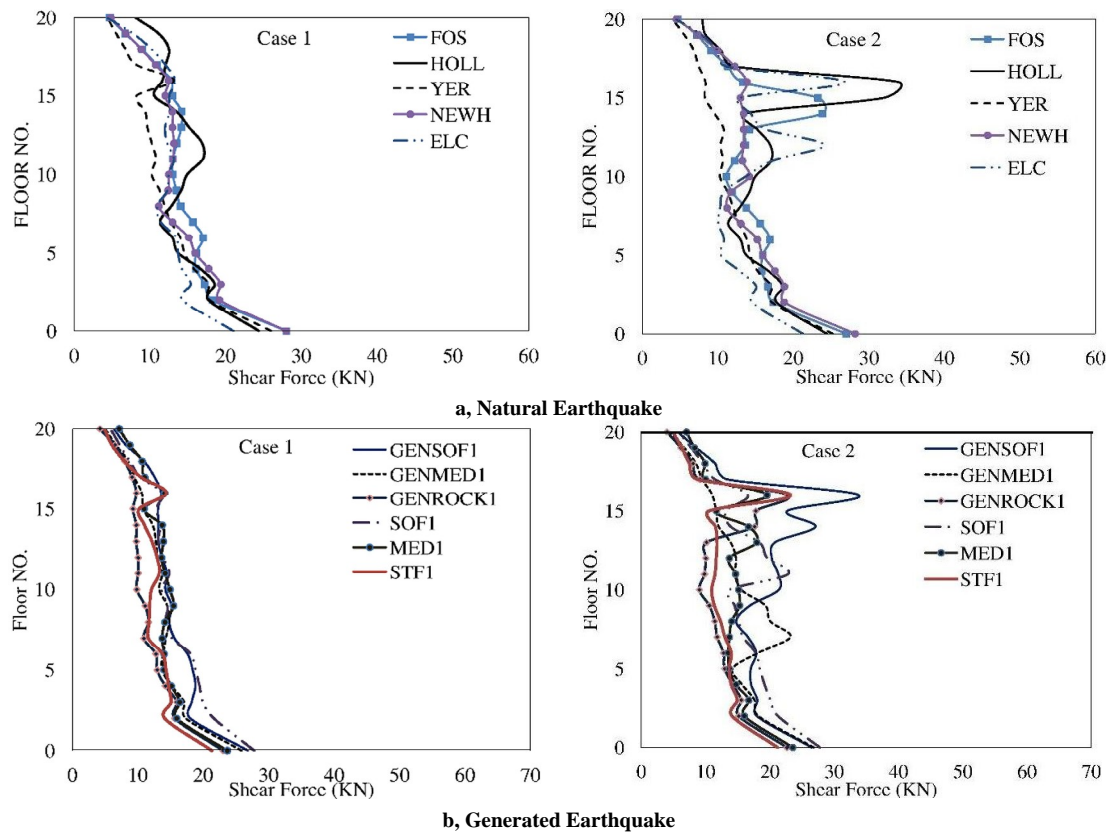


Fig. 6- End Column Shear Force for Group G_{20-15} Due to Selected Earthquake

4- CONCLUSIONS

Based on the results of the analytical investigation conducted in this study, the following key points are noted;

* Pounding mainly affects shear forces, which increase suddenly above and below the positions of pounding.

* Floor-to-column collision is the worst case of pounding problem, which often leads to buildings collapse.

* Floor-to-column pounding during earthquakes makes the end column shear distributions along buildings height is non-uniform and chaotic.

* The value of end column shear force due to pounding between adjacent buildings for buildings constructed on soft soil is larger than those constructed on medium or rock soil.

* Floor-to-column pounding during earthquake makes the maximum end column shear located below the positions of pounding, which is not found at the base as expected in the design of individual buildings.

* The maximum roof displacement of adjacent buildings differs for the different earthquakes even though they have the same peak ground acceleration. This means that the required separation distances to prevent or minimize pounding between adjacent buildings can not only be controlled through considering the peak ground acceleration without regard to the ground motion caused by the earthquake. In other words, a safe gap distance cannot be specified without regard to the structural system of the two adjacent buildings.

* Since the behaviour of each building's geometry was not similar to the others, each case of adjacent building should be analysed according to its own conditions.

* It is noted that the building configurations presented above are not optimized to cause diaphragm oscillation; thus other building configurations may show significantly more dependence on mass distribution. Research is ongoing onto other building configurations and their sensitivity to mass distribution.

5- REFERENCES

- 1- AbdelRaheem, S.E. [2006] "Seismic pounding between adjacent building structures", *Electronic Journal of Structural Engineering* 6, 66-74.
- 2- Anagnostopoulos, S.A. [1988] "Pounding of buildings in series during earthquakes", *Earthquake Engineering and Structural Dynamics* 16, 443-456.
- 3- Anagnostopoulos, S.A. [1992] "An Investigation of earthquake induced pounding between adjacent buildings", *Earthquake Engineering and Structural Dynamics* 21, 289-302.
- 4- Clough, R., and Penzien, T. [1993] *Dynamic of Structures*, MCGraw-Hill, Inc.
- 5- Cole, G., Dhakal, R., Carr, A., and Bull, D. [2010] "An investigation of the effects of mass distribution on pounding structures", *Earthquake Engineering and Structural Dynamics* 10, 1002-1052.
- 6- ECP Committee 203 [2007] "The Egyptian code for design and construction of concrete structures", *Housing and Building Research Centre, Giza, Egypt*.
- 7- Jankowski, R. [2005] "Non-linear viscoelastic modelling of earthquake-induced structural pounding", *Earthquake Engineering and Structural Dynamics* 34, 595-611.
- 8- Karayannis, C. G. And Favvata, M. J. [2005] "Earthquake-induced interaction between adjacent reinforced concrete structures with non-equal heights". *Earthquake Engineering and Structural Dynamics* 34, 1-20.

- 9- Maison, B.F. and Kasai, K. [1990] "Analysis for type of structural pounding", *Journal of Structural Engineering*, 116(4), 957-975.
- 10- Matsagar, V.A. and Jangid, R.S. [2005] "Viscoelastic damper connected to adjacent structures involving seismic isolation", *Journal of Civil Engineering and Management* 11(4), 309-322.
- 11- Mouzakis, H. P. and Papadrakakis, M. [2004] "Three dimensional nonlinear building pounding with friction during earthquakes", *Journal of Earthquake Engineering* 8, 107-132.
- 12- Muthukumar, S. And Desroches, R. [2006] "A Hertz contact model with non-linear damping for simulation", *Earthquake Engineering and Structural Dynamics* 35, 811-828.
- 13- Prakash, V., Powell, G., and Campbell, S. [1993] "DRAIN-2DX Base Program Description and User Guide; version 1.10," Report No. UBC/SEMM-93/17&18, *Structural Engineering Mechanics and Materials*, Department of Civil Engineering, University of California, Berkeley.
- 14- Rahman, A. M., Carr, A. J. and Moss, P. J. [2001] "Seismic pounding of a case of adjacent multiple-storey buildings of differing total heights considering soil flexibility effects". *Bulletin of the New Zealand Society for Earthquake Engineering*, 34:1, 40-59.
- 15- Rosenblueth, E. and Meli, R. [1986] "The 1985 earthquake: causes and effects in Mexico City", *Concrete International* 8(5), 23-34.
- 16- Sayed S. Abdel Salam, Osman Shallah, Tharwat Sakr, and Ebtsam Fathy [2005] "Pounding influence on adjacent buildings with different dynamic properties", *Proceeding of The Ninth International Colloquium on Structural and Geotechnical Engineering*, Ain Shams University, Cairo, Egypt.
- 17- Shakya, K. and Wijeyewickrema A. C. [2009] "Mid-column pounding of multi-story reinforced concrete buildings considering soil effects", *Advances in Structural Engineering* 12(1), 71-85.
- 18- Van Mier, J. G. M., Preuijssers, A. F., Reinhardt, H. W., and Monnier, T. [1991] "Load- time response of colliding concrete bodies", *Journal of Structural Engineering* 117, 354-374.
- 19- Westermo, B.D. [1989] "The Dynamics of inter structural connection to prevent pounding", *Earthquake Engineering and Structural Dynamics*, 18, 687-699.